Comparing the sensitivity of different intestinal Caco-2 in vitro monocultures and co-cultures to amorphous silicon dioxide nanomaterials and the clay montmorillonite

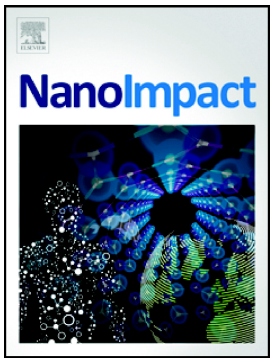

Impact of amorphous silicon dioxide nanomaterials and the nanoclay montmorillonite on intestinal Caco-2 in vitro monocultures and co-cultures

Victor C. Ude, David M. Brown, Vicki Stone, Helinor J. Johnston

PII: S2452-0748(18)30193-9
DOI: https://doi.org/10.1016/j.impact.2019.100165
Article Number: 100165
Reference: IMPACT 100165

To appear in: *NANOIMPACT*

Received date: 20 November 2018
Revised date: 4 April 2019
Accepted date: 8 May 2019

Please cite this article as: V.C. Ude, D.M. Brown, V. Stone, et al., Impact of amorphous silicon dioxide nanomaterials and the nanoclay montmorillonite on intestinal Caco-2 in vitro monocultures and co-cultures, NANOIMPACT, https://doi.org/10.1016/j.impact.2019.100165

Impact of amorphous silicon dioxide nanomaterials and the nanoclay Montmorillonite on intestinal Caco-2 *in vitro* monocultures and co-cultures

Victor C. Ude*, David M. Brown, Vicki Stone, Helinor J. Johnston*

Nano Safety Research Group, School of Engineering and Physical Sciences, Institute of Biological Chemistry, Biophysics and Bioengineering, Heriot-Watt University, Edinburgh, EH14 4AS, UK.

Authors address: All the authors share the same address as stated above and individual e-mail addresses are as follows:

Victor C. Ude: victor_chibueze@yahoo.co.uk

David Brown: d.brown@hw.ac.uk

Vicki Stone: v.stone@hw.ac.uk

*Corresponding author: Dr. Helinor Johnston, Nano Safety Research Group, School of Engineering and Physical Sciences, Institute of Biological Chemistry, Biophysics and Bioengineering, Heriot-Watt University, Edinburgh, EH14 4AS, UK. Tel: +44 (0)131 451 3303. E-mail: h.johnston@hw.ac.uk

[1]

[1] **Abbreviations**

ANOVA, Analysis of variance; **DCFH-DA,** 2',7'-Dichlorofluorescin diacetate; **EDTA**, Ethylenediaminetetraacetic acid; **ELISA**, Enzyme-Linked Immuno-Sorbent Assay; **FBS**, Fetal bovine serum; **IL-8**, Interleukin-8; **MMT,** Montmorillonite; **PBS**, Phosphate buffered saline; **ROS,** Reactive oxygen species; **SiO_2,** Silicon dioxide; **TEER**, Transepithelial electrical potential.

Abstract

Nanomaterials (NMs) including the nanoclay montmorillonite (MMT) and silicon oxide (SiO_2) are exploited in diverse health and consumer products that may lead to their ingestion. There is a lack of studies on the toxicity of SiO_2 NMs and MMT using intestinal *in vitro* models. Here, we investigate the toxicity of SiO_2 NMs and MMT nanoclays to the intestine using four intestinal *in vitro* models via assessment of cytotoxicity, transepithelial electrical resistance (TEER), cell morphology reactive oxygen species (ROS) and interleukin (IL)-8 production. SiO_2 NMs and MMT were non-toxic when cell viability, TEER and cell morphology were assessed as indicators of toxicity, across all models. SiO_2 NMs and MMT did not stimulate production of ROS in acellular and cellular conditions. IL-8 was stimulated by only SiO_2 NMs and the level produced was low, which may not be biologically significant. Using a battery of tests, it was identified that SiO_2 NMs and MMT are relatively non-toxic. However, comparison of the results with *in vivo* data would identify which *in vitro* models provide a good prediction of NM toxicity to inform testing strategies for assessment of the toxicity of ingested NMs and to ensure the safe use of food relevant NMs in future.

Keywords: Montmorillonite, Silicon dioxide, ingestion, interleukin -8, TEER.

1. Introduction

The gastrointestinal (GI) tract is a complex barrier-exchange system and a boundary between the external environment and the systemic environment of the human body. The GI tract is formed from a range of cell types, with different structures and functions including; enterocytic (epithelial) cells, endocrine cells, Paneth cells, goblet cells, and microfold cells (Madara, 2011). The surface area of the intestine is increased by the presence of villi and microvilli (Helander and Fändriks, 2014). The microbiome is a community of bacteria that resides in the GI tract and contributes to several GI tract functions (Jandhyala et al., 2015), The major cell type of the GI tract is enterocytes. Enterocytes are tightly sealed by tight junctions, which prevent the translocation of substances from the intestinal lumen to the systemic environment (Landy et al., 2016). A compromise in tight junction function leads to inflammation and enhanced penetration of toxic compounds and pathogens to the systemic environment (Ma et al., 2012; Schulzke et al., 2009). *In vitro*, the function of tight junctions is monitored by performing permeability studies (using insulin or mannitol) and via measurement of transepithelial electrical resistance (TEER). TEER measures the ability of the cell monolayer to separate ionic charge across the epithelia, and intestinal monolayers are termed leaky or tight based on their electrical resistance (Ma et al., 2012). However, to my knowledge, there is published paper which has studied the toxicity of silicon dioxide (SiO_2) NMs and montmorillonite (MMT) in the intestine *in vitro* using differentiated Caco-2 cells and intestinal co-culture models via TEER measurements.

Microfold cells represent ~10 % of the follicle-associated epithelium and are responsible for luminal antigen sampling (Gamboa and Leong, 2013; Jepson and Ann Clark, 1998; Jepson and Clark, 2001; Lefebvre et al., 2015). M cells lack microvilli in the apical side and are responsible for particles and pathogens transport across the intestinal epithelium to the underlying immune cells (Brayden et al., 2005; Corr et al., 2008; des Rieux et al., 2007;

Jepson and Clark, 2001; Shakweh et al., 2004). M cells function as antigen sampling cells and are a site for microbial and particulate matter trafficking (Powell et al., 2007).

The intestinal epithelium lined with mucus, is secreted by the goblet cells and functions as a first line of defence against invading pathogens, essential for digestion and absorption of food including egestion of undigested food, microorganisms and its by-products (Kim and Ho, 2010; Pelaseyed et al., 2014). Mucus prevents infection and activation of inflammation, clearing and separating toxic materials such as pathogens from the epithelial cells to protect the intestinal epithelium (Hansson, 2012).

The human Caco-2 cell line is widely accepted for *in vitro* toxicity studies and was first isolated from a human colon adenocarcinoma (Fogh et al., 1977). Caco-2 cells spontaneously differentiate to a mature human intestinal epithelium after culturing for 15-21 days (Natoli et al., 2011; Sambuy et al., 2005; Sambuy et al., 2001). Undifferentiated Caco-2 cells lack some biochemical and morphological characteristics of human enterocytes, but they represent proliferating cells (Tarantini et al., 2015b), hence they depict more closely the intestinal crypt epithelial cells. Differentiated Caco-2 cells share many morphological and functional characteristics of enterocytes *in vivo*, such as the presence of microvilli, functional tight junctions joining the cells in the monolayer, expression of characteristic hydrolases such as sucrose-isomaltase, lactase, aminopeptidase N and dipeptidyl peptidase IV of the absorptive enterocytes of small intestine (Ferruzza et al., 2012; Sambuy et al., 2001). Differentiated Caco-2 cells lack a mucus layer and microfold (M) cells, but Caco-2 cells can be used to develop co-culture models, which incorporate these cells. Co-culturing of differentiated Caco-2 and HT29-MTX cells in a transwell plate leads to the development of a mucus secreting *in vitro* intestinal model (Sambuy et al., 2001). This model has been used to study the toxicity and intestinal transport of substances across the intestinal epithelium (Georgantzopoulou et al., 2016; Kavanaugh et al., 2013; Martínez-Maqueda et al., 2015;

Sigurdsson et al., 2013; Yuan et al., 2013). Caco-2/HT29-MTX co-culture has not been used to investigate the toxicity of SiO_2 NMs and MMT.

There are currently three different *in vitro* models of M cells and all involve seeding of Caco-2 cells into the apical (AP) compartment of a transwell plate, and the Raji B cell line or murine lymphocytes into the basolateral (BL) compartment. The first model is a co-culture of murine lymphocytes from the Peyer's patches and Caco-2 cells where Caco-2 cells are seeded into the AP compartment of the transwell plates and cultured for 14 days and murine lymphocytes from the Peyer's patches are seeded in the BL compartment and grown for 4 to 6 days (Kernéis et al., 1997). The second model is a co-culture of human Burkitt's Raji B cells and Caco-2 cells, where Raji B cells are seeded in the BL compartment of the transwell plate after 14 days and are grown for a further 4-6 days (des Rieux et al., 2005). The third model involves a co-culture of Caco-2 cells and Raji B cells but the insert is inverted 3-5 days post seeding of Caco-2 cells and Raji B cells seeded after 14 days and are cultured for 4-6 days then the inserts are placed back at its original orientation (des Rieux et al., 2007). The toxicity of SiO_2 NMs and MMT has not been studied using any of these three types of *in vitro* M cell models.

The most wildly synthesised NM globally is SiO_2 (Decan et al., 2016). SiO_2 NMs are used by various sectors in diverse products. For example, SiO_2 NMs are used in biomedical applications for drug delivery, bio imaging and cancer therapy (Kim et al., 2015; Pasqua et al., 2009; Sakai-Kato et al., 2014; Schübbe et al., 2012). In addition, SiO_2 NMs are used in biotechnology for DNA transfection and in a range of consumer products such as cosmetics, drugs, paints, and food as a food additive (anti-caking agent) (Decan et al., 2016; McCracken et al., 2013), and in agriculture for gene delivery in plants (Decan et al., 2016). SiO_2 NMs are also used to maintain the flow of powder in a range of products (e.g. vending machine powders, milk and cream powder substitutes, cheese and sugar) (Smolkova et al., 2015). The

use of silica NMs in this range of products may lead to human exposure via ingestion, inhalation, dermal, adsorption and injection. A series of toxicology studies have been conducted with different type of silica. *In vitro* (using cell lines) have investigated the toxicity of SiO_2 NMs to the lungs, intestine and skin and the available results are often contradictory. For example, cytotoxicity, ROS production and modified gene expression (CAT, GSTA4, TNF-α, CYP1A, POR, SOD1, GSTM3, GPX1, and GSR1) were exhibited by food grade silica (10-50 nm) after exposure to WI-38 cells (human lung normal fibroblasts) for 24 or 48 h (Athinarayanan et al., 2014). Decan et al also observed a loss of viability after exposure of lung epithelial cells (FE1 cells) to SiO_2 NMs (5 -20 nm) (Decan et al., 2016). Assessment of cytotoxicity, genotoxicity and nuclear localization of SiO_2 NMs (12-200 nm) exposed to undifferentiated and differentiated Caco-2 cells demonstrated a non-toxic effect after 5, 24, 48 and 72 h exposure (Gerloff et al., 2013; McCracken et al., 2016; McCracken et al., 2013; Sakai-Kato et al., 2014; Schübbe et al., 2012). However, IL-8 secretion was observed after undifferentiated Caco-2 cells were exposed to SiO_2 NMs (15 nm) at highest concentration (32 µg/ml) whereas 55 nm sized SiO_2 NMs did not induce IL-8 production (Tarantini et al., 2015b). The findings suggest that the physicochemical properties of SiO_2 NMs influence their toxicity, and that different cell types vary in their sensitivity to SiO_2 NM toxicity. *In vivo* studies have demonstrated that SiO_2 NMs (10-22 nm) are non-toxic after oral gavage, intratracheal instillation and intravenous administration to rats (Guichard et al., 2015; Hofmann et al., 2015; Tarantini et al., 2015a). Although, induction of IL-8 by SiO_2 has been assessed, there is no published paper on the assessment of the toxicity of SiO_2 via measurement of TEER and light microscopy post staining of the exposed cell with Romanowisky stain.

Nanoclays are a form of layered minerals silicates, which could be natural or synthetic and are used in a diverse array of products. Different types of natural nanoclays exist

(montmorillonite (MMT), bentonite, zeolite, kaolinite, chlorite, halloysite palygorskite and sepiolite) (Chu and Garwood, 1992; Papoulis, 2011), but MMT is the most widely used nanoclay in health and industrial formulations (Baek et al., 2012; Sharma et al., 2010), hence the reason for selection of MMT for the study.

MMT is a layered material that has a large specific surface area, high cation exchange capacity, high adsorption properties and adhesive ability (Aguzzi et al., 2007; Baek et al., 2012; Maisanaba et al., 2015; Mallakpour and Dinari, 2011; Papoulis, 2011). These properties of MMT are usually harnessed for pharmaceutical uses such as drug delivery and protection of bioactive substances against harsh degradation in a biological environment (Aguzzi et al., 2007; Papoulis, 2011). MMT can also be used for food packaging materials due to its antimicrobial characteristics and impact on gas permeability (Maisanaba et al., 2015; Thomas et al., 2012).

Existing studies suggest that MMT is relatively non-toxic. MMT has been shown to induce cytotoxic effects, only at very high concentration (125 μg/ml) after 72 h exposure to human INT-407 intestinal cells (derived from HeLa cell line) whereas no toxicity was observed after oral administration of up to 1,000 mg/kg to mice (Baek et al., 2012). An increase in TNF-α, IL-6 and LDH secretion but there was an absence of micronucleus formation (indicator of genotoxicity) in A549 lung epithelial cells after exposure to MMT (200 μg/ml) (Huo et al., 2015). Other researchers have also demonstrated a non-toxic effect after exposure of MMT to undifferentiated Caco-2 cells, with only organically modified MMT capable of inducing a cytotoxic effect via reactive oxygen species (ROS) production, glutathione increase and DNA damage (comet assay) (Maisanaba et al., 2014; Sharma et al., 2010). This implies that the toxicity of MMT is a result of the organic modification. Cu/Zn loaded MMT induced an increase in TEER *ex vivo*, anti-inflammatory cytokine (TGF-β1) mRNA expression, and protein levels, and downregulation of TNFα, IL6, IL8 and IL1β mRNA expression in the

intestine of weaned piglets after 21 days feeding of a mixture of basal diet and 2 g/kg Cu/Zn loaded MMT (Lefei et al., 2017). However, the difference between these published papers is that the toxicity of MMT was not studied using intestinal *in vitro* models. Therefore, the toxicity of undifferentiated and differentiated Caco-2 cells which have less physiological similarity to the in vivo intestine compared to co-cultures were not compared in previous studies.

Due to a lack of published papers on impact of MMT and SiO_2 NMs on the intestine and the anticipated increase in the ingestion of MMT and SiO_2 NMs there is the need to investigate their toxicity to the intestine using simple and complex intestinal *in vitro* models. Therefore, the toxicity of SiO_2 NMs and MMT were assessed in four *in vitro* intestinal models (undifferentiated Caco-2 cells, differentiated Caco-2 cells, Caco-2/HT29-MTX and Caco-2/Raji B co-cultures) using TEER measurement, cytotoxicity, cell morphology (light microscopy) and IL-8 production. It was hypothesized that SiO_2 and MMT will induce more toxicity to the Caco-2 monocultures than the co-culture models. By using a battery of tests to assess NM toxicity and by employing a variety of *in vitro* models of varied complexity, a comprehensive assessment of SiO_2 and MMT toxicity will be performed. The information obtained can be used to provide an evidence base for decision making purposes (e.g. to inform the selection of NMs to use in products, risk management), and to inform which *in vitro* models are prioritised when assessing NM toxicity to the intestine in the future.

2. Materials and methods

2.1. Nanomaterials

Synthetic amorphous silicon dioxide (SiO_2) NMs, also known as NM-202, was provided by the Fraunhofer Institute of Molecular Biology and Applied Ecology (IME, Germany) as a powder. These SiO_2 NMs have been characterised by the European Commission's Joint

Research Centre (JRC) Repository in Ispra, Italy (http://ihcp.jrc.ec.europa.eu/our_activities/nanotechnology/nanomaterials-repository). The primary particle size of SiO_2 NMs, has been measured previously with TEM and ranged between 5 and 30 nm, with evidence that the NMs can agglomerate to a size ranging between 10 and 600 nm. The specific surface area of the SiO_2 NMs was 184.0 m^2/g (Cotogno et al., 2013; Rasmussen et al., 2013). MMT was provided as a kind gift from BYK (BYK additive and instrument Manchester, UK). The size of MMT was not provided by the supplier and due to its layered nature, it was not possible to measure its size with a scanning or transmission electron microscope.

2.2. Nanomaterial preparation

MMT and SiO_2 NMs were dispersed by modifying the procedure developed by (Jacobsen et al., 2010). Briefly, the MMT nanoclay was suspended in Mili Q H_2O to obtain a 1 mg/ml stock suspension, which was vortexed for 30 sec. and then mixed for 1 h with a Dynal sample mixer (MXIC1, 18 RPM) fetal bovine serum (FBS) was then added to give a final concentration of 2 % FBS in the suspension. SiO_2 NMs were dispersed in 2 % FBS in Milli Q de-ionised water at a concentration of 1mg/ml. The MMT nanoclay and SiO_2 suspensions were then sonicated for 16 min in a bath sonicator without pause. Following the sonication step, all samples were used immediately. After sonication the required concentration for each experiment was obtained by serial dilution in the appropriate cell culture medium. To determine the acute toxicity of MMT and SiO_2 NMs, 10 concentrations of the NMs were prepared and ranged between 0.37 to 78.13 $\mu g/cm^2$ (equivalent to 1.17 to 250 µg/ml).

2.4. Dynamic light scattering analysis

The hydrodynamic diameter, zeta potential and polydispersity index (PdI) of SiO_2 NMs and MMT nanoclay were measured in biological media (MEM and DMEM complete cell culture

medium) using dynamic light scattering (DLS) (Malvern Zetasizer Nano series). SiO_2 NMs and MMT were prepared as described above and the concentration was adjusted to 100 µg/ml via dilution in phenol red free cell culture medium supplemented with 10 % FBS, 100 U/ml penicillin/streptomycin, 100 IU/ml NEAA, and 2 mM L-glutamine). The hydrodynamic diameter, PdI and Zeta potential of the samples were measured in triplicate at 0 h and at 24 h (following incubation at 37 °C).

2.5. Cell culture

The human colon colorectal adenocarcinoma Caco-2 cell line and Human Burkitti's lymphoma; B lymphocyte (Raji B) cell line were obtained from the American Type Culture Collection (ATCC) (USA). The HT29-MTX clone E-12 cell line was obtained from the European Collection of Authentic Cell Culture (ECACC) (UK). Caco-2 and HT29-MTX cells were maintained in 4.5 g/l glucose Dulbecco's modified eagle medium (DMEM) (Sigma) supplemented with 10 % heat inactivated FBS (Gibco Life Technologies), 100 U/ml Penicillin/Streptomycin (Gibco Life Technologies), 100 IU/ml NEAA (Gibco Life Technologies), and 2 mM L- glutamine (Gibco Life Technologies) (termed DMEM complete cell culture medium), at 37 ºC and 5 % CO_2 and 95 % humidity. Raji B cells were maintained in Roswell Park Memorial Institute (RPMI) 1640 Medium (Gibco Life Technologies) supplemented with 10 % heat inactivated FBS (Gibco Life Technologies), 100 U/ml Penicillin/Streptomycin (Gibco Life Technologies) (termed RPMI complete cell culture medium) and at 37 ºC, 5 % CO_2 and 95 % humidity.

Differentiated Caco-2 cells were cultured on 3.0 µm pore polycarbonate transwell inserts in a 12 well plate with a growth area of 1.12 cm^2 (Costar corning, Flintshire, UK). Cells were seeded at a concentration of 3.13 x 10^5 cells/cm^2 (500 µl/well) in DMEM complete cell culture medium into the AP compartment of the transwell insert, and the BL compartment was filled with 1.5 ml of DMEM complete cell culture medium. The cells were cultured at 37

^{o}C, 5 % CO_2 and 95 % humidity for 18-21 days. The medium was changed every other day for the first 16 days and then every day until 21 days.

The Caco-2/Raji B co-culture (M cell model) of the gastrointestinal epithelium was cultivated by modifying the protocol previously described by (des Rieux et al., 2005; Gullberg et al., 2000; Schimpel et al., 2014). Briefly, 3.13 x 10^5 cells/cm^2 of Caco-2 cells were suspended in 0.5 ml of DMEM complete cell culture medium and seeded into the AP compartment of 3.0 µm pore polycarbonate transwell inserts in a 12- well plate, with a growth area of 1.12 cm^2 (Corning) and grown for 15 days at 37 ^{o}C, 5 % CO_2 and 95 % humidity. The medium in both the AP (0.5 ml) and BL (1.5 ml) compartments was changed every other day. On the 15th day, 5 x 10^5 cells/ml of Raji B cells were suspended in DMEM complete cell culture medium (1.5 ml) and seeded into the BL compartment. The co-culture was grown for 5 days under standard incubation conditions and the medium was changed only in the AP compartment every day.

The Caco-2/HT29-MTX co-culture (mucus secreting) model of the gastrointestinal epithelium was cultured by modifying the protocol of (Georgantzopoulou et al., 2016; Pan et al., 2015). Briefly, 3.13 x 10^5 cells/cm^2 of Caco-2 and HT29-MTX cells were seeded into the AP compartment of 3.0 µm pore polycarbonate transwell inserts in a 12-well plate with a growth area of 1.12 cm^2 (Costar corning, Flintshire, UK) at a ratio of 9:1. The co-culture was maintained in 4.5 g/l glucose DMEM complete cell culture medium. The cells were cultivated at 37 ^{o}C, 5 % CO_2 and 95 % humidity for 20-21 days and the medium changed every other day for the first 16 days and then every day until the 21st day. The differentiation status of differentiated Caco-2 cells, Caco-2/Raji B and Caco-2/HT29-MTX co-cultures was confirmed via measurement of TEER, tight junction staining and via visualisation of microvilli using Scanning Electron Microscopy (SEM) as described previously (Ude et al.,

2017). Only cell models with TEER values greater than 500 $\Omega.cm^2$ were used for experiments.

2.6. Alamar blue cell viability assay

The viability of undifferentiated Caco-2 cells exposed to SiO_2 NMs and MMT was assessed via the Alamar blue assay. Caco-2 cells were seeded at a concentration of 1.56 x 10^5 cells /cm^2 into a 96 well plate (surface area 0.32 cm^2) (Costar Corning Flintshire UK) and incubated at 37 ºC and 5 % CO_2 for 24 h. The cells were then washed twice with PBS (Gibco Life Technologies) and exposed to 100 µl of MEM complete cell culture medium (negative control), 0.1 % triton-X 100 (positive control), and SiO_2 NMS or MMT at concentrations ranging from 0.37 to 78.13 µg/cm^2. After 24 h, the cells were washed twice with PBS and exposed to 100 µl of Alamar blue reagent (0.1 mg/ml in MEM complete cell culture medium) (Sigma, Poole). The cells were incubated for 4 h at 37 ºC, 5 % CO_2 and fluorescence measured with a microplate reader (SpectraMax M5) at a wavelength of 560/590 nm (excitation/emission). Data are expressed as mean % viability (i.e. % of the negative control).

2.7. Evaluation of acellular and intracellular ROS production

Acellular ROS production by SiO_2 NMs and MMT was investigated by modifying the methods described by Foucaud et al. (2007) and Sauvain et al. (2013). Briefly, 10 mM DCFH-DA (2',7'-Dichlorofluorescin diacetate in methanol) was hydrolysed by diluting 10 mM DCFH-DA to a concentration of 1 mM in methanol and then to 0.2 mM in 0.01M NaOH. The solution was incubated at RT for 30 min in the dark and 0.1M PBS (pH 7.4) was then added to stop the reaction (to give a concentration of 0.05 mM DCF). The reaction mixture was then placed on ice and used immediately. As a control, an equivalent volume of 0.01 M NaOH, 0.1 M PBS (pH 7.4) and methanol was prepared without DCFH-DA. The

DCFH reaction mixture or the mixture without DCFH-DA was transferred to the wells of a black clear bottomed 96 well plate (225 µl/well) in triplicate. This was followed by the addition of 25 µl of MEM complete cell culture medium without phenol red (negative control), 7.81 or 15.63 µg/cm^2 of SiO_2 or MMT and 1mM of H_2O_2 (positive control) (in complete MEM cell culture medium without phenol red). The fluorescence generated by DCF oxidation was measured at time zero and 2 h at 485/530 nm (ex/em) with constant shaking at RT. Data are expressed as mean fold change (compared to the control).

For cellular ROS production, undifferentiated Caco-2 cells (1.56 x10^5 cells /cm^2) were grown in a 96 well plate (Costar Corning) and maintained at 37 ^{o}C, 5 % CO_2 and 95 % humidity for 24 h. Cells were then washed twice with PBS and 150 µM of DCFH-DA (in Hanks' Balanced Salt Solution (HBSS)) was added (100 µl). The cells were then incubated for 1 h in the dark at 37 ^{o}C, 5 % CO_2 and 95 % humidity. Next, the cells were washed with PBS and exposed to HBSS (untreated control), 7.81, 15.63 or 31.25 µg/cm^2 of SiO_2 NMs or MMT and 1mM H_2O_2 (positive control) diluted in HBSS and incubated at 37 ^{o}C, 5 % CO_2 and 95 % humidity. The fluorescent readings were taken at 0 h and 2 h at a wavelength of 485/530 nm (excitation/emission) using a SpectraMax M5 (California USA) microplate reader, Data are expressed as mean fold change, compared to the control.

2.8. Investigation of the impact of SiO_2 NMs and MMT on intestinal cell barrier integrity using TEER measurement

TEER was measured after exposure of differentiated Caco-2 cells, and the Caco-2/HT29-MTX and Caco-2/Raji B co-cultures to DMEM complete cell culture medium (untreated control), 7.81 or 15.63 µg/cm^2 of SiO_2 NMs or MMT for 24 h as described in Ude et al., (2017).

Romanowsky staining: Cell morphology

Undifferentiated Caco-2 cells were seeded at a concentration of 3.13 x 10^5 cells/cm^2 and grown on a 10 mm glass coverslip in a 24 well plate (Costar Corning, Flintshire, UK) and incubated at 37 ^oC, 5 % CO_2 and 95 % humidity for 24h. Cells were then exposed to DMEM complete cell culture medium (control), 7.81 or 15.63 µg/cm^2 SiO_2 NMs or MMT for 24 h. Differentiated Caco-2 cells, Caco-2/HT29-MTX and Caco-2/Raji B co-cultures were treated with DMEM complete cell culture medium (control) and 15.63 µg/cm^2 of SiO_2 NMs or MMT for 24 h. Following exposure, cells were stained with Rapid Romanowsky stain (TCS Biosciences, England). The glass coverslips or polycarbonate inserts were mounted onto glass slides with DPX (Sigma, Poole UK) and covered with a glass coverslip. Cells were viewed and imaged using a light microscope-Zeiss fluorescent microscope, Carl Zeiss Axio Scope A 1 Upright Research Microscope (Germany) fitted with camera (ZEISS Axiocam ERc 5s) (magnification 40 X).

2.9. IL-8

The supernatant from undifferentiated Caco-2 cells exposed to DMEM complete cell culture medium (control), 7.81, 15.63 and 31.25 µg/cm^2 of SiO_2 NMs or MMT and supernatants from differentiated Caco-2 cells, Caco-2/HT29-MTX and Caco-2/Raji B co-cultures exposed to DMEM complete cell culture medium (control), 7.81 and 15.63 µg/cm^2 SiO_2 NMs or MMT for 24 h were used to assess IL-8 production using an Enzyme-Linked Immunosorbent Assay (ELISA) (R&D System, Inc., Minneapolis, MN USA) following the manufacturer's protocol. Absorbance was measured using a SpectraMax M5 microplate reader (California USA) at a wavelength of 450 nm and the IL-8 concentration in samples was calculated from the standard curve. Data are expressed as mean IL-8 concentration (pg/ml).

2.10. Data analysis

All experiments were repeated at least three times (on different days) and all data are expressed as mean ± standard error of the mean (SEM). The figures were generated using Graph Pad Prism. A one-way analysis of variance (ANOVA) with a Tukeys multiple comparison was performed, after the normality check to assess statistical significance, using Minitab 17 software.

3. Results

3.1. Characterisation of the SiO_2 and MMT

SiO_2 NMs and MMT were characterised by measuring hydrodynamic diameter, zeta potential and PdI using DLS (Table 1 and 2) after dispersion in MEM and DMEM complete cell culture medium at 0 and 24 h. The average hydrodynamic diameter of SiO_2 NMs in MEM and DMEM was 133.07 and 125.57 nm at 0 h respectively and 162.58 and 139.34 nm post 24 h incubation respectively. SiO_2 NMs were therefore agglomerated in both MEM and DMEM complete media at both time points investigated, as the primary size was between 5-30 nm (Rasmussen et al., 2013). The zeta potential of SiO_2 NM suspensions was negative, ranging from -8.61 to -10.01 mV and the PdI ranged between 0.59 and 8.3. The hydrodynamic diameter of MMT was 276.24 and 294.23 at 0 and 24 h respectively. The zeta potential was negative, ranging from -9.2 to -10.1 mV. Incubation of MMT for 24 h did not affect the zeta potential or the PdI (0.56-0.69).

	Time (h)	0	24
Complete MEM	Hydrodynamic diameter (nm)	133.07±7.80	162.58 ±5.81
	Zeta Potential (mV)	-10.01±0.30	-8.61±0.38
	PdI	0.71±0.07	0.69±0.02
Complete DMEM	Hydrodynamic diameter (nm)	125.57±10.09	139.34±12.88
	Zeta Potential (mV)	-9.28±0.50	-8.95±0.69
	PdI	0.83±0.09	0.59±0.05

Table 1: Hydrodynamic diameter, zeta potential and polydispersity index (PdI) values of SiO_2 NMs in MEM and DMEM complete cell culture medium. Data are expressed as mean ± SEM (n=3).

	Time (h)	0	24
Complete MEM	Hydrodynamic diameter (nm)	276.24±15.44	294.23±13.30
	Zeta Potential (mV)	-9.22±0.20	-10.10±0.089
	PdI	0.57±0.02	0.59±0.03
Complete DMEM	Hydrodynamic diameter (nm)	275.57±13.36	335.04±9.12
	Zeta Potential (mV)	-9.36±0.65	-10.02±0.20
	PdI	0.56±0.02	0.69±0.01

Table 2: Hydrodynamic diameter, zeta potential and polydispersity index (PdI) values of MMT in MEM and DMEM complete cell culture medium. Data are expressed as mean ± SEM (n=3).

3.2. Alamar blue cell viability assay

Viability of undifferentiated Caco-2 cells was assessed using the Alamar blue assay after treatment with SiO_2 NMs and MMT for 24 h. No loss of cell viability was observed at all concentrations tested, for both NMs (Figure 1).

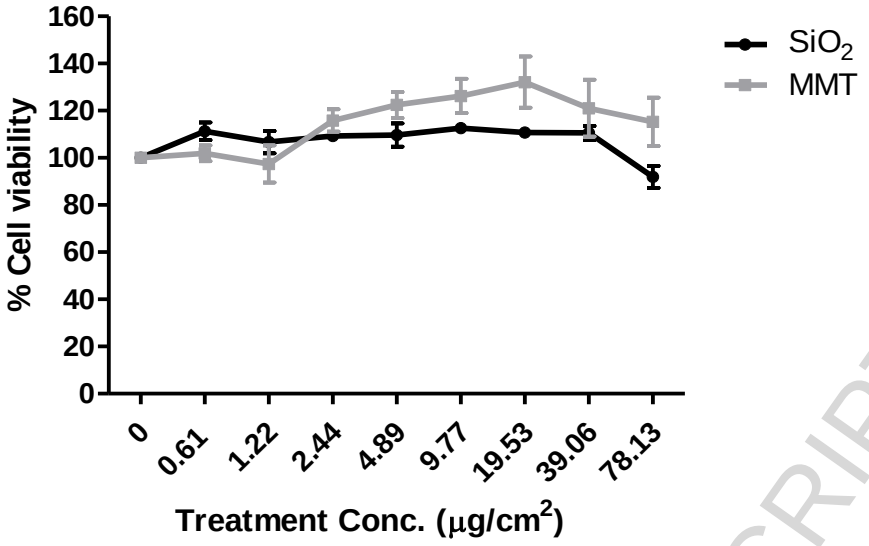

Figure 1: Cytotoxicity of SiO_2 NMs and MMT to undifferentiated Caco-2 cells.

Viability of undifferentiated Caco-2 cells was assessed using the Alamar blue assay following exposure of cells to MEM complete cell culture medium (control), SiO_2 NMs or MMT at concentrations ranging from 0.61 and 78.13 μg/cm^2 for 24 h. Viability of Caco-2 cells was assessed using the Alamar blue assay, and data are expressed as mean % of the control (i.e. % viability) ± SEM (n = 3).

3.3. ROS formation

Acellular ROS production by SiO_2 NMs and MMT was assessed via the DCFH-DA assay (Figure 2). There was no significant production of ROS by SiO_2 NMs and MMT at 2 h whereas H_2O_2 produced a significant increase in ROS (~5 fold), compared to the control.

ROS production was also assessed in undifferentiated Caco-2 cells at 2 h post exposure (Figure 3). SiO_2 NMs and MMT (at all treatment concentrations) did not stimulate ROS production. A significant increase in ROS production was observed in H_2O_2 exposed cells (Figure 3). Since SiO_2 NMs and MMT did not stimulate ROS production in acellular conditions and in undifferentiated Caco-2 cells, ROS production was not investigated in the

differentiated Caco-2 cells and the co-culture models as they are known to be less responsive to NM toxicity (e.g. Ude et al., 2017).

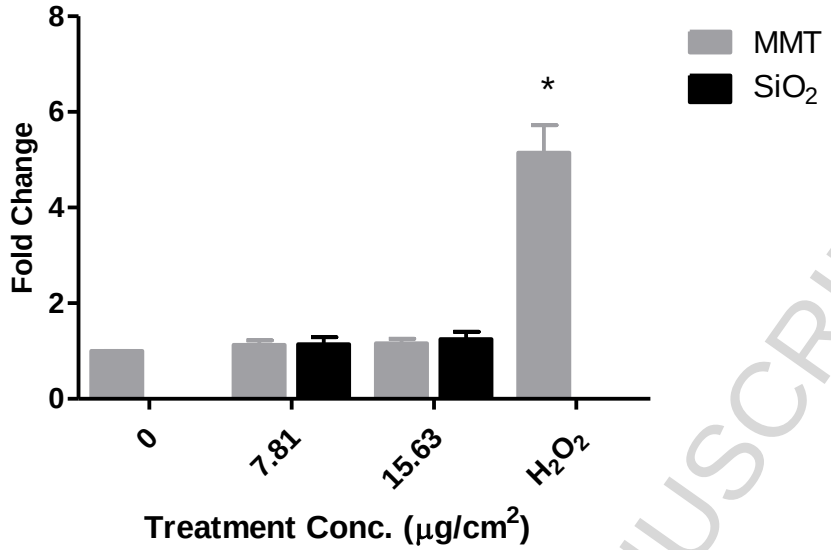

Figure 2: Acellular ROS production by SiO_2 NMs and MMT at 2 h. Acellular ROS levels were determined in cell culture medium (0), and for SiO_2 NMs and MMT at concentrations of 7.81 and 15.63 µg/cm^2 using the DCFH-DA assay at 2 h post exposure. Data are expressed as mean fold change (compared to the control) ± SEM (n = 3).

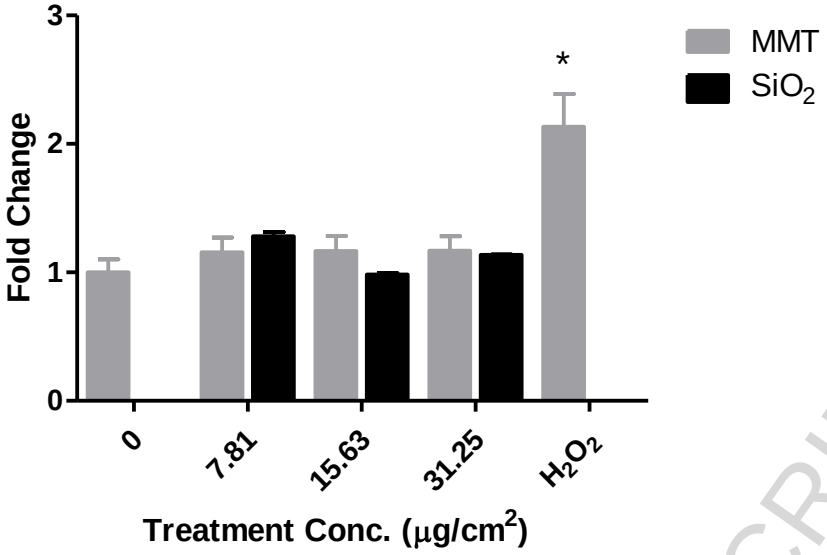

Figure 3: ROS formation by undifferentiated Caco-2 cells 2 h post exposure to SiO_2 NMs and MMT. Intracellular ROS levels were determined using the DCFH-DA assay in undifferentiated Caco-2 cells following exposure to cell culture medium (control, 0), H_2O_2, SiO_2 NMs or MMT at concentrations of 7.81, 15.63, 31.25 μg/cm^2 for 2h. Data are expressed as mean fold change (compared to the control) ± SEM (n = 3).

3.4. Impact of SiO_2 NMs and MMT on cell morphology

The impact of SiO_2 NMs and MMT on intestinal barrier integrity was investigated in differentiated Caco-2 cells, Caco-2/HT29-MTX and Caco-2/Raji B co-culture models via assessment of TEER measurement and light microscopy (Romanowisky staining). The TEER values were similar to the control following exposure of all cell models to SiO_2 NMs and MMT at all concentrations and time points (Figure 4). There was no difference in cell number and the structural morphology of undifferentiated Caco-2 cells, differentiated Caco-2 cells, Caco-2/HT29-MTX and Caco-2/Raji B co-cultures compared to control after 24 h treatment with SiO_2 NMs and MMT, suggesting that there was no loss in cell viability (Figure 5).

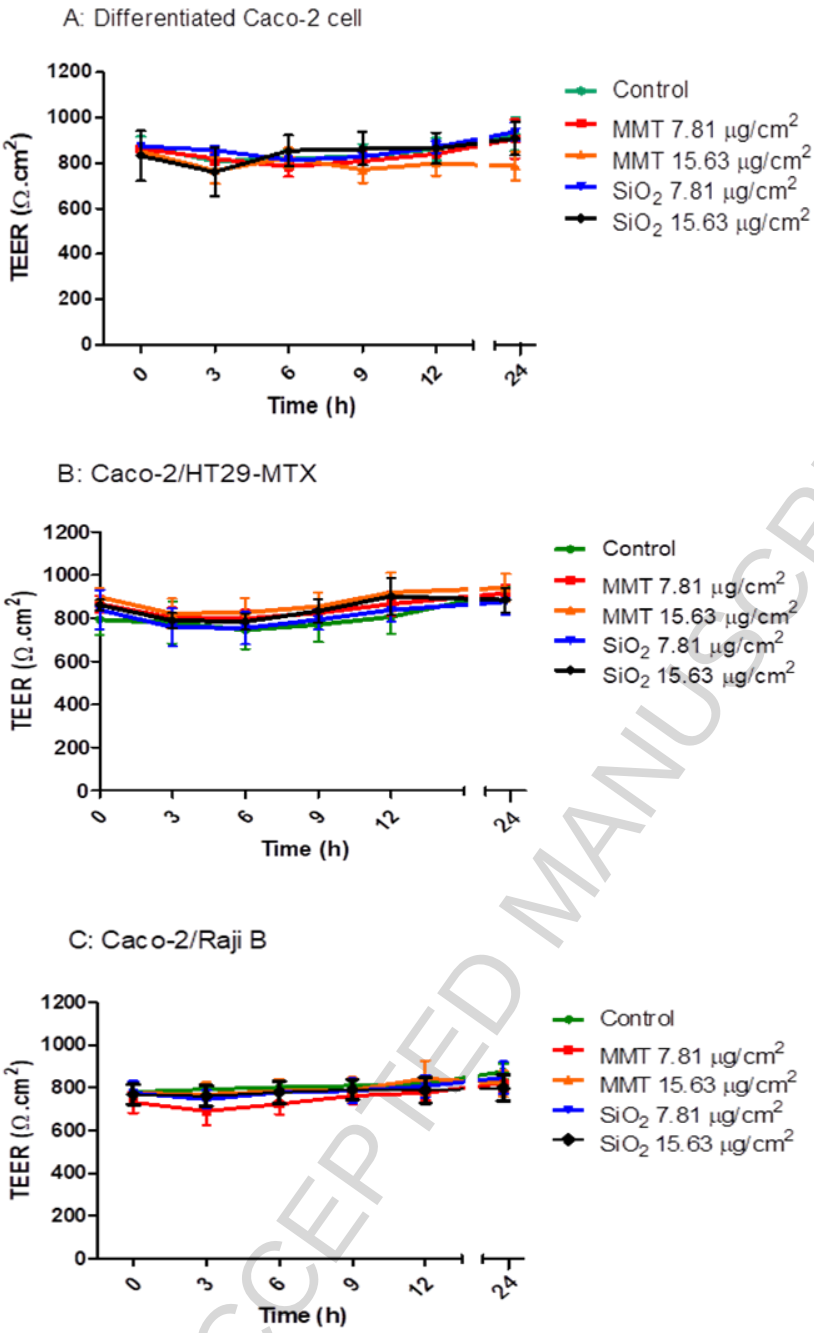

Figure 4: Impact of SiO_2 NMs and MMT on *in vitro* intestinal model TEER values. Differentiated Caco-2 cells (A), the Caco-2/HT29-MTX co-culture (B), and the Caco-2/Raji B co-culture (C) were exposed to cell culture medium (control, 0), SiO_2 NMs and MMT at concentrations of 7.81 or 15.63 µg/cm^2 for 24 h. The TEER values were measured using epithelial voltohmmeter EVOM every 3 h. Data are expressed as mean TEER value ± SEM (n = 3).

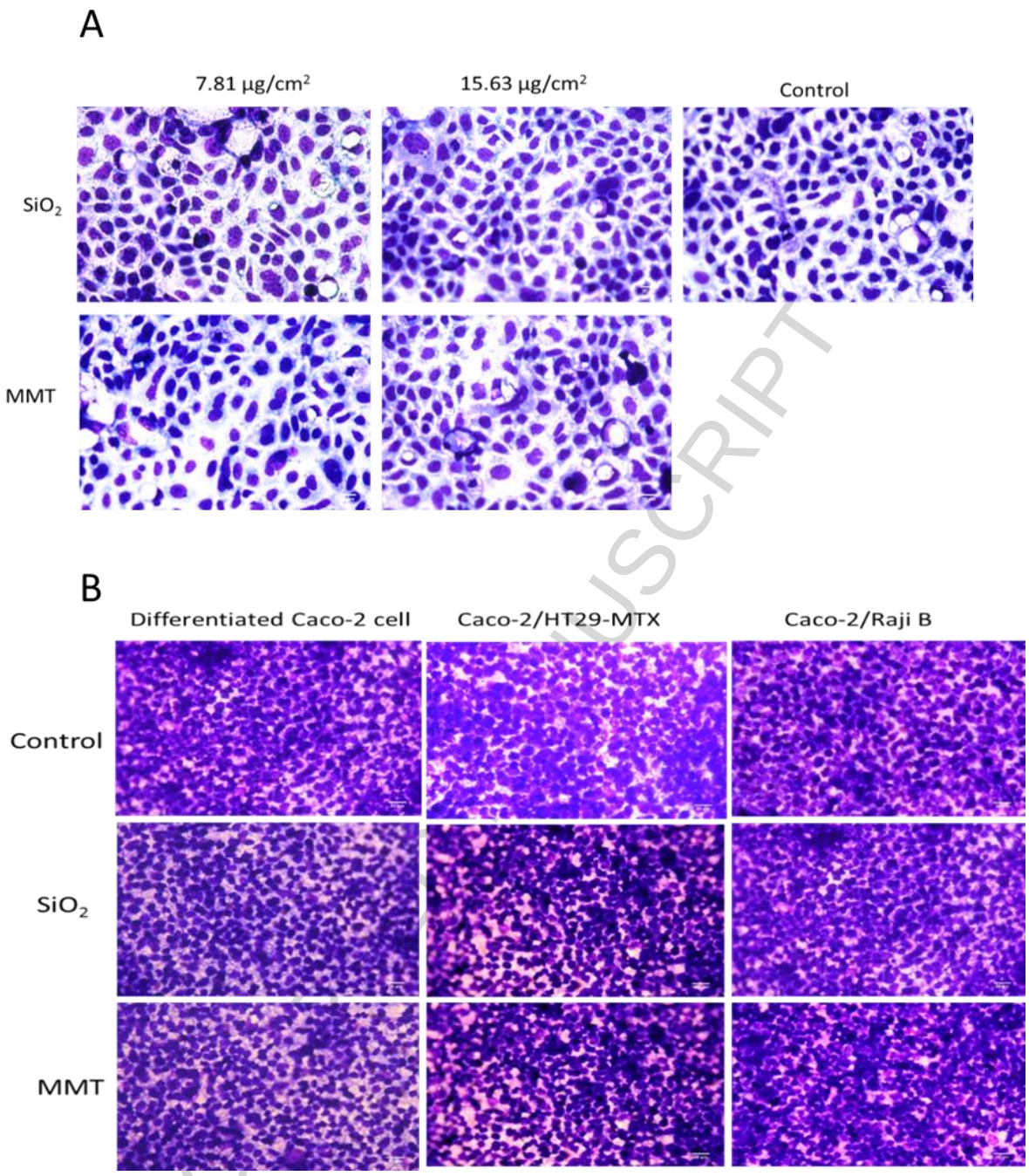

Figure 5: Impact of SiO_2 NMs and MMT on *in vitro* intestinal cell morphology. A) Undifferentiated Caco-2 cells, B) Differentiated Caco-2 cells, Caco-2/HT29-MTX and Caco-2/Raji B co-cultures were exposed to cell culture medium (control) and 7.81 or 15.63 µg/cm^2 of SiO_2 NMs or MMT and cultured for 24 h. The cells were fixed, stained and visualised using the light microscopy (magnification 40 X, scale bar=20 µm. Representative images are shown (n=3).

3.5. IL-8 production

A significant increase in IL-8 production was observed after exposure of undifferentiated Caco-2 cells to SiO_2 NMs for 24 h at all concentrations compared to control which was below detectable limit by ELISA. In contrast IL-8 production was comparable to the control following exposure of undifferentiated Caco-2 cells to 15.63 and 31.25 µg/cm^2 of MMT (Figure 6A).

Differentiated Caco-2 cells exposed to 7.81 and 15.63 µg/cm^2 SiO_2 NMs demonstrated a significant increase in IL-8 secretion (32.91 and 31.09 pg/ml respectively), compared to control which was below detectable limit by ELISA (Figure 6B). No IL-8 production was detected following exposure of differentiated Caco-2 cells to MMT. Generally, IL-8 secretion induced by MMT and the untreated control in differentiated Caco-2 cells was below the limit of detection.

SiO_2 NMs (7.81 and 15.63 µg/cm^2) stimulated a significant increase in IL-8 production (48.55 and 69.96 pg/ml respectively) by the Caco-2/HT29-MTX co-culture at 24 h post exposure compared to control (Figure 6C). No IL-8 production from the Caco-2/HT29-MTX co-culture exposed to MMT or cell culture medium (control) was detected. (Figure 6C). The Caco-2/Raji B co-culture secreted a concentration of 57.91 and 48.13 pg/ml of IL-8 after exposure to SiO_2 NMs (at concentrations of 7.81 and 15.63 µg/cm^2 respectively). There was no detectable secretion of IL-8 by MMT and the control by the Caco-2/Raji B co-culture (Figure 6D).

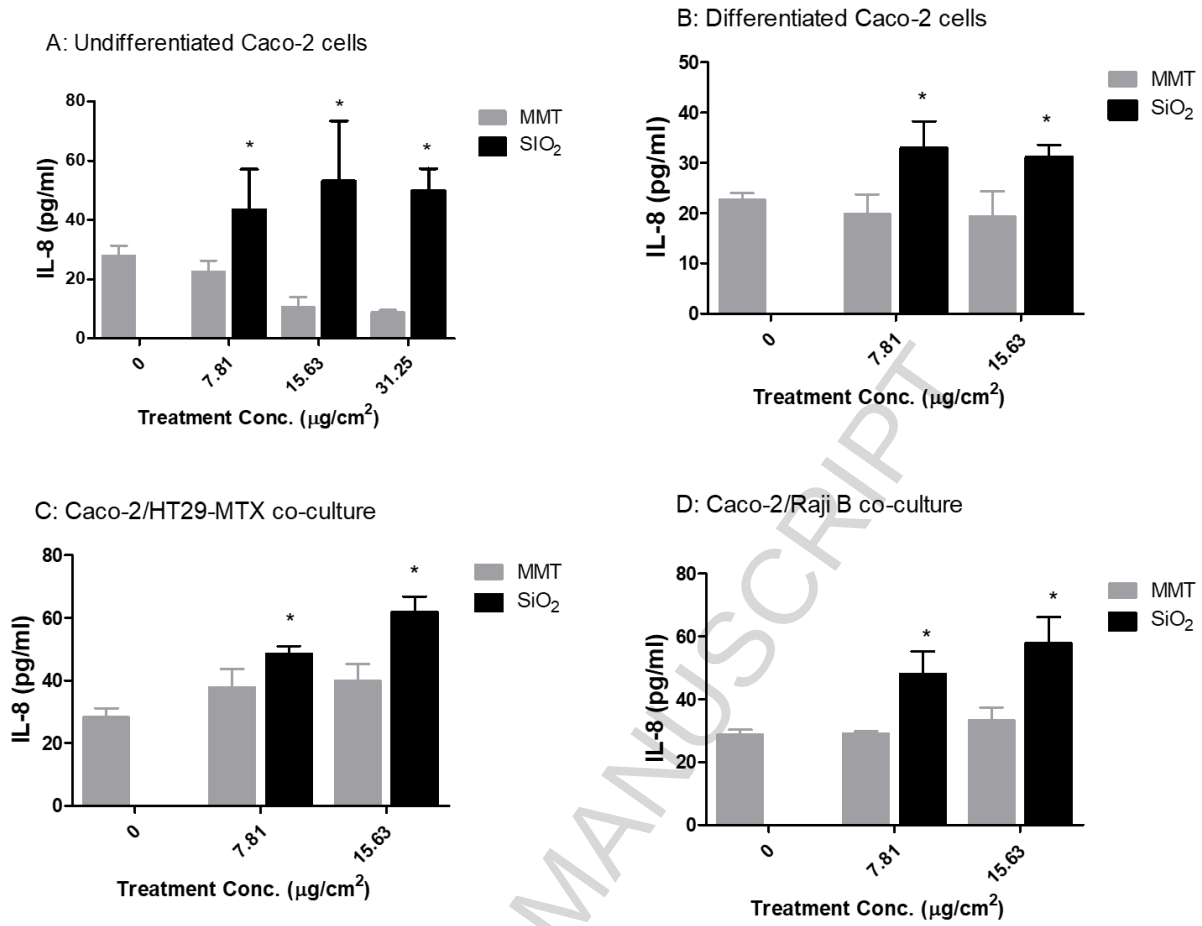

Figure 6: IL-8 production by undifferentiated Caco-2 cells, differentiated Caco-2 cells, and the Caco-2/HT29-MTX and Caco-2/Raji B co-cultures. Undifferentiated Caco-2 cells (A), differentiated Caco-2 cells (B), the Caco-2/HT29-MTX co-culture (C) and the Caco-2/Raji B co-culture (D) were exposed to cell culture medium (control, 0), SiO_2 NMs or MMT at concentrations of 7.81, 15.63 or 31.25 µg/cm^2 for 24 h. The level of IL-8 in the cell supernatant was determined using an ELISA. Data are expressed as mean IL-8 concentration (pg/ml) ± SEM (n = 3). Significance at $P<0.05$ is indicated by * compared to control.

4. Discussion

In this study the toxicity of SiO_2 NMs and MTT was assessed to a range of in vitro models of varied complexity (undifferentiated Caco-2 cells, differentiated Caco-2 cells, Caco-2/HT29-MTX and Caco-2/Raji B co-cultures), using a battery of endpoints. Obtained data suggests

that both NMs are of relatively low toxicity. The *in vitro* models employed in this study were used previously to assess the toxicity and translocation of copper oxide nanomaterials (CuO NMs) and copper sulphate ($CuSO_4$) (Ude et al., 2017, Ude et al., 2018). It was observed whilst CuO NMs and $CuSO_4$ stimulated toxicity across all models, the undifferentiated Caco-2 cells were more sensitive than the differentiated Caco-2 cells, and that the co-cultures were least sensitive (Ude et al., 2017, Ude et al., 2018).

4.1. Physicochemical properties of SiO_2 and MMT

Both SiO_2 NMs and MMT are likely to be agglomerated in the cell culture medium. The primary size of SiO_2 NMs have been shown to range between 5 and 30 nm (Rasmussen et al., 2013) indicating that SiO_2 NMs agglomerated in cell culture media. The primary size of MMT is not known as they are in layered form with a thickness of 1nm and so it was not possible to measure the size using electron microscopy. Agglomeration of synthetic amorphous SiO_2 NMs has been reported (Rasmussen et al., 2013).

4.2. Cytotoxicity and impact of SiO_2 NMs and MMT on cell morphology

The Alamar blue assay was used to assess the viability of undifferentiated Caco-2 cells after exposure to SiO_2 NMs and MMT at 24 h post exposure. Both SiO_2 NMs and MMT did not cause cytotoxicity. A similar lack of cytotoxicity has been reported of SiO_2 NMs of various physicochemical properties on undifferentiated Caco-2 cells up 72 h post exposure (Gerloff et al., 2013; McCracken et al., 2016; McCracken et al., 2013; Sakai-Kato et al., 2014; Schübbe et al., 2012). On the other hand, FE1 (human lung epithelial) and WI-38 (human fibroblast) cells demonstrated slight cytotoxicity at 24 and 48 h post exposure of Si and SiO_2 NMs (Athinarayanan et al., 2014; Decan et al., 2016). Although, the study by Athinarayanan et al used the same type of SiO_2 as used in this study, cytotoxicity assessment was performed with the MTT assay whereas this study used Alamar blue, which may explain why different results

were obtained as different viability assays vary in their sensitivity. Furthermore, different cell types are likely to differ in their susceptibility to SiO2 NM toxicity. MMT has also shown a non-toxic effect at 24 h post exposure to undifferentiated Caco-2 cells (Maisanaba et al., 2014; Sharma et al., 2010) whereas long term exposure of INT-407 cells (HeLa derived cell line) to MMT induced cytotoxicity only at high concentration (125 µg/ml) (Baek et al., 2012). Our findings are therefore in agreement with existing research and suggest that MTT is relatively non-toxic.

The toxicity of SiO_2 NMs and MMT on undifferentiated Caco-2 cells was also investigated with light microscopy after exposure to SiO_2 NMs and MMT, and these findings confirmed the findings obtained from the Alamar Blue assay.

Whilst several studies have assessed the impacts of SiO2 NMs and MTT on undifferentiated cells, as described above, a lack of studies have evaluated impacts on more complex models. The Alamar blue assay cannot be applied to differentiated Caco-2 models and co-cultures in a transwell insert, and previous studies using CuO NMs demonstrated that light microscopy provided a useful and rapid insight into the cytotoxicity of NMs (Ude et al., 2017). Therefore, light microscopy was employed to perform a direct comparison of NM cytotoxicity across different intestinal *in vitro* models. SiO_2 NMs and MMT did not impact on the confluence or morphology of the exposed cells (in all models used), compared to the control, suggesting that these NMs were not toxic. Light microscopy has not been used to study the toxicity of SiO_2 NMs and MMT in intestinal models (e.g. differentiated Caco-2 cells, Caco-2/HT29-MTX and Caco-2/Raji B co-culture) previously. However, use of light microscopy to assess toxicity of NMs has been used for other cell types. For example, the toxicity of Ag NMs, ufCB and TiO_2 to differentiated HL-60 neutrophil- like cells has been studied using light microscopy and change in a cell morphology and reduced cell viability was observed after exposure to Ag NMs and ufCB (Johnston et al. 2015). Reduction in cell number and viability

was also observed after exposure of CuO NMs and CuSO4 to undifferentiated Caco-2 cells (Ude et al., 2017). Therefore, whilst light microscopy does not provide a quantitative assessment of NM cytotoxicity, and has not been commonly used to assess the response of Caco-2 cells to NMs previously it is a rapid and cost-effective method that can be used to explore the impact of NMs on cell viability and morphology, and it is therefore recommended that it is used more commonly to assess NM toxicity *in vitro*.

TEER measurement was also used to assess the integrity of the intestinal barrier in differentiated Caco-2 cells, Caco-2/HT29-MTX and Caco-2/Raji B co-cultures after exposure to SiO_2 NMs and MMT. No impact on TEER value was observed after exposure to SiO_2 NMs and MMT compared to control suggesting that SiO_2 NMs and MMT were not toxic at the exposed concentrations. In contrast, exposure of CuO NMs and $CuSO_4$ to differentiated Caco-2 cells caused a concentration and time dependent reduction in the TEER value compared to control (Ude et al., 2017). In addition, Cu/Zn loaded MMT exposed to the intestine of weaned piglets has been shown to increase in TEER value *ex vivo* (Lefei et al., 2017) suggesting that Cu/Zn loaded MMT was not toxic at the test concentration. There are no published papers that have studied the toxicity of SiO_2 NMs and MMT to the intestine *in vitro* by measuring the TEER values. However a decrease in TEER has been reported after exposure of CuO, Ag, TiO_2 and polystyrene NMs to differentiated Caco-2 cells (Piret et al., 2012), Caco-2/HT29-MTX (Brun et al., 2014; Walczak et al., 2015) and the Caco-2/Raji B co-culture (Bouwmeester et al., 2011; Lozoya-Agullo et al., 2017). However, in previous studies TEER was only measured at one-time point, making their study different from this present study. Measurement of TEER values maximises the amount of information obtained for one measurement of toxicity study, therefore it is recommended that future studies continue to assess TEER over time as an indicator of NM toxicity.

4.3. ROS production

Since stimulation of oxidative stress is known as key mechanism underlying NM toxicity (Abbott Chalew and Schwab, 2013; Abdal Dayem et al., 2017; Fu et al., 2014; Johnston et al., 2010; Onodera et al., 2015), acellular and cellular ROS production by SiO_2 NMs and MMT was assessed via the DCFH-DA assay. SiO_2 NMs did not produce ROS in acellular conditions and undifferentiated Caco-2 cells. Similar results were reported after exposure of human gastric epithelial cells (GES-1) and undifferentiated Caco-2 cells to SiO_2 NMs (10-50 nm) (Kaiser et al., 2013; Tarantini et al., 2015b; Yang et al., 2014). However, ROS production has been stimulated by SiO2 NMs in human lung fibroblast cells (Athinarayanan et al., 2014). ROS formation was also mediated in A549 and HepG2 epithelial cells and NIH/3T3 fibroblasts at post 24 h exposure to different sizes of SiO_2 NMs (20, 60, 100 and 200 nm) and 100 and 200 nm SiO_2 NMs generated greater ROS compared to 20 and 60 nm (Kim et al., 2015). These findings therefore indicate that SIO2 NMs may stimulate cell dependent toxicity. Of interest is that SiO_2 NMs (14 nm) induced acellular ROS production when assessed in artificial digested and undigested form using Electron Paramagnetic Resonance (EPR) (Gerloff et al., 2013). Therefore, the physicochemical properties of SiO_2 NMs are likely to influence whether they stimulate ROS production in acellular and acellular conditions.

MMT also demonstrated no increase in acellular and cellular ROS with the DCFH-DA assay in this study. Absence of acellular and cellular ROS production after exposure up to 170 µg/ml of MMT to undifferentiated Caco-2 cells for 24 h has also been reported (Sharma et al., 2010). However, an increase in ROS production after exposure of 40 µg/ml of MMT to undifferentiated Caco-2 cells has also been demonstrated, at 24 and 48 h post exposure (Maisanaba et al., 2014) however, the MMT concentration were higher than the concentration used in this present study.

Previous studies demonstrated that ROS production stimulated by CuO NMs and CuSO4 was greater in undifferentiated Caco-2 cells than differentiated Caco-2 cells and co-cultures (Ude et al., 2017, 2018). Therefore, due to an absence of ROS production by SiO2 NMs and MTT in undifferentiated Caco-2 cells (in our study and those of the wider scientific community) ROS production was not assessed in the differentiated cells and co-cultures.

4.4. IL-8 production

IL-8 production is one of the prominent markers used for the study of NM toxicity in intestinal *in vitro* models. SiO_2 NMs exposed to undifferentiated Caco-2 cells, differentiated Caco-2 cells, Caco-2/HT29-MTX and Caco-2/Raji B co-cultures for 24 h induced IL-8 production at all concentrations tested. Although SiO_2 NMs stimulated IL-8 secretion was statistically significant, it is unlikely to be biologically significant as only a relatively small increase in cytokine production was observed.

There are conflicting findings in the literature about whether SiO_2 stimulates IL-8 production from cells *in vitro*. For example, Tarantini et al. (2015b) reported a similar level of IL-8 production to this study after exposure of 32 µg/ml of SiO_2 NMs (15 nm) to undifferentiated Caco-2 cells, with a lack of induction of IL-8 by lower concentrations and at all concentrations of larger SiO_2 NMs (55 nm), indicating a size and concentration dependent IL-8 release. Another researcher reported a lack of IL-8 expression by undifferentiated and differentiated Caco-2 cells after exposure to SiO_2 NMs (14 nm) (Gerloff et al., 2013). In contrast, an increase in IL-8 secretion has been reported after exposure of A549 monoculture and A549/THP-1 co-cultures to SiO_2 NMs (10 to 60 nm) (Choi et al., 2009; Wottrich et al., 2004). Normal mesothelial cells (MET-5A) exposed to both nano and micro silica particles also demonstrated an increase in IL-8 secretion (Brown et al., 2007). This suggests that IL-8 release after exposure to SiO_2 NMs may be cell dependent, as Caco-2 cells seem to have lower response compared to the other cell types.

In this study, MMT did not stimulate IL-8 release 24 h post exposure to undifferentiated Caco-2 cells, differentiated Caco-2 cells, Caco-2/HT29-MTX and Caco-2/Raji B co-culture. Lefei et al. (2017) reported a decrease in mRNA expression of pro-inflammatory cytokines such as TNFα, IL6, IL8 and IL1β after oral exposure of copper/zinc-loaded montmorillonite to weaned piglets *in vivo*. MMT induced a significant increase in IL-6 after exposure of A549 lung epithelial cells (Huo et al., 2015). The level of cytokine produced are unlikely to be physiologically relevant as small levels of IL-8 were produced in all the intestinal models.

5. Conclusions

SiO_2 NMs and MMT were non-toxic to undifferentiated Caco-2 cells when toxicity was assessed via the Alamar blue assay, light microscopy, and ROS formation. In addition, SiO_2 NMs and MMT did not elicit toxicity to differentiated Caco-2 cells, Caco-2/HT29-MTX and Caco-2/Raji B co-cultures when light microscopy, and TEER was used to assess toxicity. Whilst SiO_2 NMs stimulated IL-8 release in all the intestinal *in vitro* models, no IL-8 secretion was induced by MMT. These findings can be used to inform the testing strategy used to assess the toxicity of ingested NMs in the future (e.g. model and endpoint selection), and by providing information on the toxicity of food relevant NMs can be used to inform the safe use of NMs in products (e.g. decision making about NM use).

Consent for publication

All authors have given their consent for the paper to be published.

Competing interests

All authors declare that they have no competing interests.

Acknowledgements

We thank Vice Chancellor of Enugu State University of Science and Technology Enugu Nigeria for granting Victor Chibueze Ude study leave and Tertiary Education Trust Fund Nigeria for paying his PhD tuition fees. We also thank BYK additive and instrument Manchester, UK for providing us with montmorillonite clay.

Availability of data and materials

Data supporting the findings are presented within the manuscript. Raw data files are available on request to the corresponding author.

References

Abbott Chalew, T.E., Schwab, K.J., 2013. Toxicity of commercially available engineered nanoparticles to Caco-2 and SW480 human intestinal epithelial cells. Cell biology and toxicology 29, 101-116.

Abdal Dayem, A., Hossain, M.K., Lee, S.B., Kim, K., Saha, S.K., Yang, G.-M., Choi, H.Y., Cho, S.-G., 2017. The Role of Reactive Oxygen Species (ROS) in the Biological Activities of Metallic Nanoparticles. International journal of molecular sciences 18, 120.

Aguzzi, C., Cerezo, P., Viseras, C., Caramella, C., 2007. Use of clays as drug delivery systems: Possibilities and limitations. Applied Clay Science 36, 22-36.

Athinarayanan, J., Periasamy, V.S., Alsaif, M.A., Al-Warthan, A.A., Alshatwi, A.A., 2014. Presence of nanosilica (E551) in commercial food products: TNF-mediated oxidative stress and altered cell cycle progression in human lung fibroblast cells. Cell biology and toxicology 30, 89-100.

Baek, M., Lee, J.-A., Choi, S.-J., 2012. Toxicological effects of a cationic clay, montmorillonite in vitro and in vivo. Molecular & Cellular Toxicology 8, 95-101.

Bouwmeester, H., Poortman, J., Peters, R.J., Wijma, E., Kramer, E., Makama, S., Puspitaninganindita, K., Marvin, H.J.P., Peijnenburg, A.A.C.M., Hendriksen, P.J.M., 2011. Characterization of Translocation of Silver Nanoparticles and Effects on Whole-Genome Gene Expression Using an In Vitro Intestinal Epithelium Coculture Model. ACS Nano 5, 4091-4103.

Brayden, D.J., Jepson, M.A., Baird, A.W., 2005. Keynote review: Intestinal Peyer's patch M cells and oral vaccine targeting. Drug Discovery Today 10, 1145-1157.

Brown, S.C., Kamal, M., Nasreen, N., Baumuratov, A., Sharma, P., Antony, V.B., Moudgil, B.M., 2007. Influence of shape, adhension and simulated lung mechanics on amorphous silica nanoparticle toxicity. Advanced Powder Technology 18, 69-79.

Brun, E., Barreau, F., Veronesi, G., Fayard, B., Sorieul, S., Chanéac, C., Carapito, C., Rabilloud, T., Mabondzo, A., Herlin-Boime, N., Carrière, M., 2014. Titanium dioxide nanoparticle impact and translocation through ex vivo, in vivo and in vitro gut epithelia. Particle and fibre toxicology 11, 13.

Choi, S.-J., Oh, J.-M., Choy, J.-H., 2009. Toxicological effects of inorganic nanoparticles on human lung cancer A549 cells. Journal of Inorganic Biochemistry 103, 463-471.

Chu, P., Garwood, W.E., 1992. Zeolite-clay composition and uses thereof. Google Patents.

Corr, S.C., Gahan, C.C., Hill, C., 2008. M-cells: origin, morphology and role in mucosal immunity and microbial pathogenesis. FEMS immunology and medical microbiology 52, 2-12.

Cotogno, G., Gibson, P., Per Axel Clausen, P.-J.d., Temmerman, S.H.N., Ceccone, G., 2013. Synthetic Amorphous Silicon Dioxide (NM-200, NM-201, NM-202, NM-203, NM-204): Characterisation and Physico-Chemical Properties In: NM-Series of Representative

Manufactured Nanomaterials. Ispra, Italy: Joint Research Centre of the European Commission.

Decan, N., Wu, D., Williams, A., Bernatchez, S., Johnston, M., Hill, M., Halappanavar, S., 2016. Characterization of in vitro genotoxic, cytotoxic and transcriptomic responses following exposures to amorphous silica of different sizes. Mutation Research/Genetic Toxicology and Environmental Mutagenesis 796, 8-22.

des Rieux, A., Fievez, V., Theate, I., Mast, J., Preat, V., Schneider, Y.J., 2007. An improved in vitro model of human intestinal follicle-associated epithelium to study nanoparticle transport by M cells. European journal of pharmaceutical sciences 30, 380-391.

des Rieux, A., Ragnarsson, E.G., Gullberg, E., Preat, V., Schneider, Y.J., Artursson, P., 2005. Transport of nanoparticles across an in vitro model of the human intestinal follicle associated epithelium. European journal of pharmaceutical sciences : 25, 455-465.

Ferruzza, S., Rossi, C., Scarino, M.L., Sambuy, Y., 2012. A protocol for in situ enzyme assays to assess the differentiation of human intestinal Caco-2 cells. Toxicology in vitro 26, 1247-1251.

Fogh, J., Fogh, J.M., Orfeo, T., 1977. One Hundred and Twenty-Seven Cultured Human Tumor Cell Lines Producing Tumors in Nude Mice. J Natl. Cancer Inst. 59, 221-226.

Foucaud, L., Wilson, M.R., Brown, D.M., Stone, V., 2007. Measurement of reactive species production by nanoparticles prepared in biologically relevant media. Toxicology letters 174, 1-9.

Fu, P.P., Xia, Q., Hwang, H.-M., Ray, P.C., Yu, H., 2014. Mechanisms of nanotoxicity: Generation of reactive oxygen species. Journal of Food and Drug Analysis 22, 64-75.

Gamboa, J.M., Leong, K.W., 2013. In vitro and in vivo models for the study of oral delivery of nanoparticles. Advanced Drug Delivery Reviews 65, 800-810.

Georgantzopoulou, A., Serchi, T., Cambier, S., Leclercq, C.C., Renaut, J., Shao, J., Kruszewski, M., Lentzen, E., Grysan, P., Eswara, S., Audinot, J.-N., Contal, S., Ziebel, J., Guignard, C., Hoffmann, L., Murk, A.J., Gutleb, A.C., 2016. Effects of silver nanoparticles and ions on a co-culture model for the gastrointestinal epithelium. Particle and fibre toxicology 13, 9.

Gerloff, K., Pereira, D.I.A., Faria, N., Boots, A.W., Kolling, J., Förster, I., Albrecht, C., Powell, J.J., Schins, R.P.F., 2013. Influence of simulated gastrointestinal conditions on particle-induced cytotoxicity and interleukin-8 regulation in differentiated and undifferentiated Caco-2 cells. Nanotoxicology 7, 353-366.

Guichard, Y., Maire, M.A., Sébillaud, S., Fontana, C., Langlais, C., Micillino, J.C., Darne, C., Roszak, J., Stępnik, M., Fessard, V., 2015. Genotoxicity of synthetic amorphous silica nanoparticles in rats following short-term exposure, part 2: Intratracheal instillation and intravenous injection. Environmental and molecular mutagenesis 56, 228-244.

Gullberg, E., Leonard, M., Karlsson, J., Hopkins, A.M., Brayden, D., Baird, A.W., Artursson, P., 2000. Expression of Specific Markers and Particle Transport in a New Human Intestinal M-Cell Model. Biochemical and Biophysical Research Communications 279, 808-813.

Hansson, G.C., 2012. Role of mucus layers in gut infection and inflammation. Current opinion in microbiology 15, 57-62.

Hayles, J., Johnson, L., Worthley, C., Losic, D., 2017. 5 - Nanopesticides: a review of current research and perspectives A2 - Grumezescu, Alexandru Mihai, New Pesticides and Soil Sensors. Academic Press, pp. 193-225.

Helander, H.F., Fändriks, L., 2014. Surface area of the digestive tract – revisited. Scandinavian Journal of Gastroenterology 49, 681-689.

Hofmann, T., Schneider, S., Wolterbeek, A., van de Sandt, H., Landsiedel, R., van Ravenzwaay, B., 2015. Prenatal toxicity of synthetic amorphous silica nanomaterial in rats. Reproductive Toxicology 56, 141-146.

Huo, T., Dong, F., Wang, M., Sun, S., Deng, J., Zhang, Q., Yu, S., 2015. Cytotoxicity of Quartz and Montmorillonite in Human Lung Epithelial Cells (A549), in: F. Dong (Ed.), Proceedings of the 11th International Congress for Applied Mineralogy (ICAM). Springer International Publishing, Cham, pp. 159-171.

Jacobsen, N.R., Pojano, G., Wallin, H., Jensen, K.A., 2010. Nanomaterial dispersion protocol for toxicological studies in ENPRA. Internal ENPRA Project Report. The National 885 Research Centre for the Working Environment.

Jandhyala, S.M., Talukdar, R., Subramanyam, C., Vuyyuru, H., Sasikala, M., Reddy, D.N., 2015. Role of the normal gut microbiota. World Journal of Gastroenterology : WJG 21, 8787-8803.

Jepson, M.A., Ann Clark, M., 1998. Studying M cells and their role in infection. Trends in Microbiology 6, 359-365.

Jepson, M.A., Clark, M.A., 2001. The role of M cells in Salmonella infection. Microbes and Infection 3, 1183-1190.

Johnston, H., Brown, D.M., Kanase, N., Euston, M., Gaiser, B.K., Robb, C.T., Dyrynda, E., Rossi, A.G., Brown, E.R., Stone, V., 2015. Mechanism of neutrophil activation and toxicity elicited by engineered nanomaterials. Toxicology in vitro :29, 1172-1184.

Johnston, H.J., Hutchison, G., Christensen, F.M., Peters, S., Hankin, S., Stone, V., 2010. A review of the in vivo and in vitro toxicity of silver and gold particulates: Particle attributes and biological mechanisms responsible for the observed toxicity. Critical reviews in toxicology 40, 328-346.

Kaiser, J.-P., Roesslein, M., Diener, L., Wick, P., 2013. Human Health Risk of Ingested Nanoparticles That Are Added as Multifunctional Agents to Paints: an In Vitro Study. PloS one 8, e83215.

Kavanaugh, D.W., O'Callaghan, J., Buttó, L.F., Slattery, H., Lane, J., Clyne, M., Kane, M., Joshi, L., Hickey, R.M., 2013. Exposure of Bifidobacterium longum subsp. infantis to Milk Oligosaccharides Increases Adhesion to Epithelial Cells and Induces a Substantial Transcriptional Response. PloS one 8, e67224.

Kernéis, S., Bogdanova, A., Kraehenbuhl, J.-P., Pringault, E., 1997. Conversion by Peyer's Patch Lymphocytes of Human Enterocytes into M Cells that Transport Bacteria. Science 277, 949-952.

Kim, I.-Y., Joachim, E., Choi, H., Kim, K., 2015. Toxicity of silica nanoparticles depends on size, dose, and cell type. Nanomedicine: Nanotechnology, Biology and Medicine 11, 1407-1416.

Kim, Y.S., Ho, S.B., 2010. Intestinal Goblet Cells and Mucins in Health and Disease: Recent Insights and Progress. Current Gastroenterology Reports 12, 319-330.

Landy, J., Ronde, E., English, N., Clark, S.K., Hart, A.L., Knight, S.C., Ciclitira, P.J., Al-Hassi, H.O., 2016. Tight junctions in inflammatory bowel diseases and inflammatory bowel disease associated colorectal cancer. World journal of gastroenterology 22, 3117-3126.

Lefebvre, D.E., Venema, K., Gombau, L., Valerio, L.G., Jr., Raju, J., Bondy, G.S., Bouwmeester, H., Singh, R.P., Clippinger, A.J., Collnot, E.M., Mehta, R., Stone, V., 2015.

Utility of models of the gastrointestinal tract for assessment of the digestion and absorption of engineered nanomaterials released from food matrices. Nanotoxicology 9, 523-542.

Lefei, J., Chun Chun, W., Huan, W., Rong, G., Fang Hui, L., Jie, F., Caihong, H., 2017. Copper/zinc-loaded montmorillonite influences intestinal integrity, the expression of genes associated with inflammation, TLR4–MyD88 and TGF-β1 signaling pathways in weaned pigs after LPS challenge. Innate Immunity 23, 648-655.

Lozoya-Agullo, I., Araújo, F., González-Álvarez, I., Merino-Sanjuán, M., González-Álvarez, M., Bermejo, M., Sarmento, B., 2017. Usefulness of Caco-2/HT29-MTX and Caco-2/HT29-MTX/Raji B Coculture Models To Predict Intestinal and Colonic Permeability Compared to Caco-2 Monoculture. Molecular pharmaceutics 14, 1264-1270.

Ma, T.Y., Anderson, J.M., Turner, J.R., 2012. Chapter 38 - Tight Junctions and the Intestinal Barrier A2 - Johnson, Leonard R, in: F.K. Ghishan, J.D. Kaunitz, J.L. Merchant, H.M. Said, J.D. Wood (Eds.), Physiology of the Gastrointestinal Tract (Fifth Edition). Academic Press, Boston, pp. 1043-1088.

Madara, J.L., 2011. Functional morphology of epithelium of the small intestine. Comprehensive Physiology.

Maisanaba, S., Gutiérrez-Praena, D., Pichardo, S., Moreno, F.J., Jordá, M., Cameán, A.M., Aucejo, S., Jos, Á., 2014. Toxic effects of a modified montmorillonite clay on the human intestinal cell line Caco-2. Journal of Applied Toxicology 34, 714-725.

Maisanaba, S., Prieto, A.I., Pichardo, S., Jordá-Beneyto, M., Aucejo, S., Jos, Á., 2015. Cytotoxicity and mutagenicity assessment of organomodified clays potentially used in food packaging. Toxicology in Vitro 29, 1222-1230.

Mallakpour, S., Dinari, M., 2011. Preparation and characterization of new organoclays using natural amino acids and Cloisite Na+. Applied Clay Science 51, 353-359.

Martínez-Maqueda, D., Miralles, B., Recio, I., 2015. HT29 Cell Line, in: K. Verhoeckx, P. Cotter, I. López-Expósito, C. Kleiveland, T. Lea, A. Mackie, T. Requena, D. Swiatecka, H. Wichers (Eds.), The Impact of Food Bioactives on Health: in vitro and ex vivo models. Springer International Publishing, Cham, pp. 113-124.

McCracken, C., Dutta, P.K., Waldman, W.J., 2016. Critical assessment of toxicological effects of ingested nanoparticles. Environmental Science: Nano 3, 256-282.

McCracken, C., Zane, A., Knight, D.A., Dutta, P.K., Waldman, W.J., 2013. Minimal Intestinal Epithelial Cell Toxicity in Response to Short- and Long-Term Food-Relevant Inorganic Nanoparticle Exposure. Chemical Research in Toxicology 26, 1514-1525.

Natoli, M., Leoni, B.D., D'Agnano, I., D'Onofrio, M., Brandi, R., Arisi, I., Zucco, F., Felsani, A., 2011. Cell growing density affects the structural and functional properties of Caco-2 differentiated monolayer. Journal of cellular physiology 226, 1531-1543.

Onodera, A., Nishiumi, F., Kakiguchi, K., Tanaka, A., Tanabe, N., Honma, A., Yayama, K., Yoshioka, Y., Nakahira, K., Yonemura, S., Yanagihara, I., Tsutsumi, Y., Kawai, Y., 2015. Short-term changes in intracellular ROS localisation after the silver nanoparticles exposure depending on particle size. Toxicology Reports 2, 574-579.

Pan, F., Han, L., Zhang, Y., Yu, Y., Liu, J., 2015. Optimization of Caco-2 and HT29 co-culture in vitro cell models for permeability studies. International Journal of Food Sciences and Nutrition 66, 680-685.

Papoulis, D., 2011. Clay-based Nanocomposites Possibilities and Limitations. AIP Conference Proceedings 1389, 1450-1453.

Pasqua, L., Cundari, S., Ceresa, C., Cavaletti, G., 2009. Recent Development, Applications, and Perspectives of Mesoporous Silica Particles in Medicine and Biotechnology. Current Medicinal Chemistry 16, 3054-3063.

Pelaseyed, T., Bergström, J.H., Gustafsson, J.K., Ermund, A., Birchenough, G.M.H., Schütte, A., van der Post, S., Svensson, F., Rodríguez-Piñeiro, A.M., Nyström, E.E.L., Wising, C., Johansson, M.E.V., Hansson, G.C., 2014. The mucus and mucins of the goblet cells and enterocytes provide the first defense line of the gastrointestinal tract and interact with the immune system. Immunological reviews 260, 8-20.

Piret, J.P., Vankoningsloo, S., Mejia, J., Noel, F., Boilan, E., Lambinon, F., Zouboulis, C.C., Masereel, B., Lucas, S., Saout, C., Toussaint, O., 2012. Differential toxicity of copper (II) oxide nanoparticles of similar hydrodynamic diameter on human differentiated intestinal Caco-2 cell monolayers is correlated in part to copper release and shape. Nanotoxicology 6, 789-803.

Powell, J.J., Thoree, V., Pele, L.C., 2007. Dietary microparticles and their impact on tolerance and immune responsiveness of the gastrointestinal tract. The British journal of nutrition 98, S59-S63.

Rasmussen, K., Mech, A., Mast, J., De Temmerman, P., Waegeneers, N., Van Steen, F., Pizzolon, J.C., De Temmerman, L., Van Doren, E., Jensen, K.A., 2013. Synthetic Amorphous Silicon Dioxide (NM-200, NM-201, NM-202, NM-203, NM-204). Characterisation and Physico-Chemical Properties. JRC Scientific and Policy Reports.

Sakai-Kato, K., Hidaka, M., Un, K., Kawanishi, T., Okuda, H., 2014. Physicochemical properties and in vitro intestinal permeability properties and intestinal cell toxicity of silica particles, performed in simulated gastrointestinal fluids. Biochimica et Biophysica Acta (BBA) - General Subjects 1840, 1171-1180.

Sambuy, Y., De Angelis, I., Ranaldi, G., Scarino, M.L., Stammati, A., Zucco, F., 2005. The Caco-2 cell line as a model of the intestinal barrier: influence of cell and culture-related factors on Caco-2 cell functional characteristics. Cell biology and toxicology 21, 1-26.

Sambuy, Y., Ferruzza, S., Ranaldi, G., De Angelis, I., 2001. Intestinal Cell Culture Models: Applications in Toxicology and Pharmacology. Cell biology and toxicology 17, 301-311.

Sauvain, J.-J., Rossi, M.J., Riediker, M., 2013. Comparison of Three Acellular Tests for Assessing the Oxidation Potential of Nanomaterials. Aerosol Science and Technology 47, 218-227.

Schimpel, C., Teubl, B., Absenger, M., Meindl, C., Fröhlich, E., Leitinger, G., Zimmer, A., Roblegg, E., 2014. Development of an Advanced Intestinal in Vitro Triple Culture Permeability Model To Study Transport of Nanoparticles. Molecular pharmaceutics 11, 808-818.

Schübbe, S., Schumann, C., Cavelius, C., Koch, M., Müller, T., Kraegeloh, A., 2012. Size-dependent localization and quantitative evaluation of the intracellular migration of silica nanoparticles in Caco-2 cells. Chemistry of Materials 24, 914-923.

Schulzke, J.D., Ploeger, S., Amasheh, M., Fromm, A., Zeissig, S., Troeger, H., Richter, J., Bojarski, C., Schumann, M., Fromm, M., 2009. Epithelial Tight Junctions in Intestinal Inflammation. Annals of the New York Academy of Sciences 1165, 294-300.

Shakweh, M., Ponchel, G., Fattal, E., 2004. Particle uptake by Peyer's patches: a pathway for drug and vaccine delivery. Expert Opinion on Drug Delivery 1, 141-163.

Sharma, A.K., Schmidt, B., Frandsen, H., Jacobsen, N.R., Larsen, E.H., Binderup, M.-L., 2010. Genotoxicity of unmodified and organo-modified montmorillonite. Mutation Research/Genetic Toxicology and Environmental Mutagenesis 700, 18-25.

Sigurdsson, H.H., Kirch, J., Lehr, C.-M., 2013. Mucus as a barrier to lipophilic drugs. International journal of pharmaceutics 453, 56-64.

Smolkova, B., El Yamani, N., Collins, A.R., Gutleb, A.C., Dusinska, M., 2015. Nanoparticles in food. Epigenetic changes induced by nanomaterials and possible impact on health. Food and Chemical Toxicology 77, 64-73.

Tarantini, A., Huet, S., Jarry, G., Lanceleur, R., Poul, M., Tavares, A., Vital, N., Louro, H., João Silva, M., Fessard, V., 2015a. Genotoxicity of synthetic amorphous silica nanoparticles in rats following short-term exposure. Part 1: Oral route. Environmental and molecular mutagenesis 56, 218-227.

Tarantini, A., Lanceleur, R., Mourot, A., Lavault, M.T., Casterou, G., Jarry, G., Hogeveen, K., Fessard, V., 2015b. Toxicity, genotoxicity and proinflammatory effects of amorphous nanosilica in the human intestinal Caco-2 cell line. Toxicology in Vitro 29, 398-407.

Thomas, S., Meera, A., Maria, H.J., 2012. Enhancing Gas-Barrier Properties of Polymer-Clay Nanocomposites. Soc. Plast. Eng. Plast. Res. Online 10.

Ude, V.C., Brown, D.M., Viale, L., Kanase, N., Stone, V., Johnston, H.J., 2017. Impact of copper oxide nanomaterials on differentiated and undifferentiated Caco-2 intestinal epithelial cells; assessment of cytotoxicity, barrier integrity, cytokine production and nanomaterial penetration. Particle and fibre toxicology 14, 31.

Ude, V.C., Brown, D.M., Viale, L., Kanase, N., Stone, V., Johnston, H.J., 2018. Using 3D gastrointestinal tract models with Microfold and mucus secreting ability to assess the hazard of copper oxide nanomaterials. Journal of Nanobiotechnology. (Submitted).

Viseras, C., Aguzzi, C., Cerezo, P., Lopez-Galindo, A., 2007. Uses of clay minerals in semisolid health care and therapeutic products. Applied Clay Science 36, 37-50.

Walczak, A.P., Kramer, E., Hendriksen, P.J.M., Tromp, P., Helsper, J.P.F.G., van der Zande, M., Rietjens, I.M.C.M., Bouwmeester, H., 2015. Translocation of differently sized and

charged polystyrene nanoparticles in in vitro intestinal cell models of increasing complexity. Nanotoxicology 9, 453-461.

Wottrich, R., Diabaté, S., Krug, H.F., 2004. Biological effects of ultrafine model particles in human macrophages and epithelial cells in mono- and co-culture. International Journal of Hygiene and Environmental Health 207, 353-361.

Yang, Y.-X., Song, Z.-M., Cheng, B., Xiang, K., Chen, X.-X., Liu, J.-H., Cao, A., Wang, Y., Liu, Y., Wang, H., 2014. Evaluation of the toxicity of food additive silica nanoparticles on gastrointestinal cells. Journal of Applied Toxicology 34, 424-435.

Yuan, H., Chen, C.-Y., Chai, G.-h., Du, Y.-Z., Hu, F.-Q., 2013. Improved Transport and Absorption through Gastrointestinal Tract by PEGylated Solid Lipid Nanoparticles. Molecular pharmaceutics 10, 1865-1873.

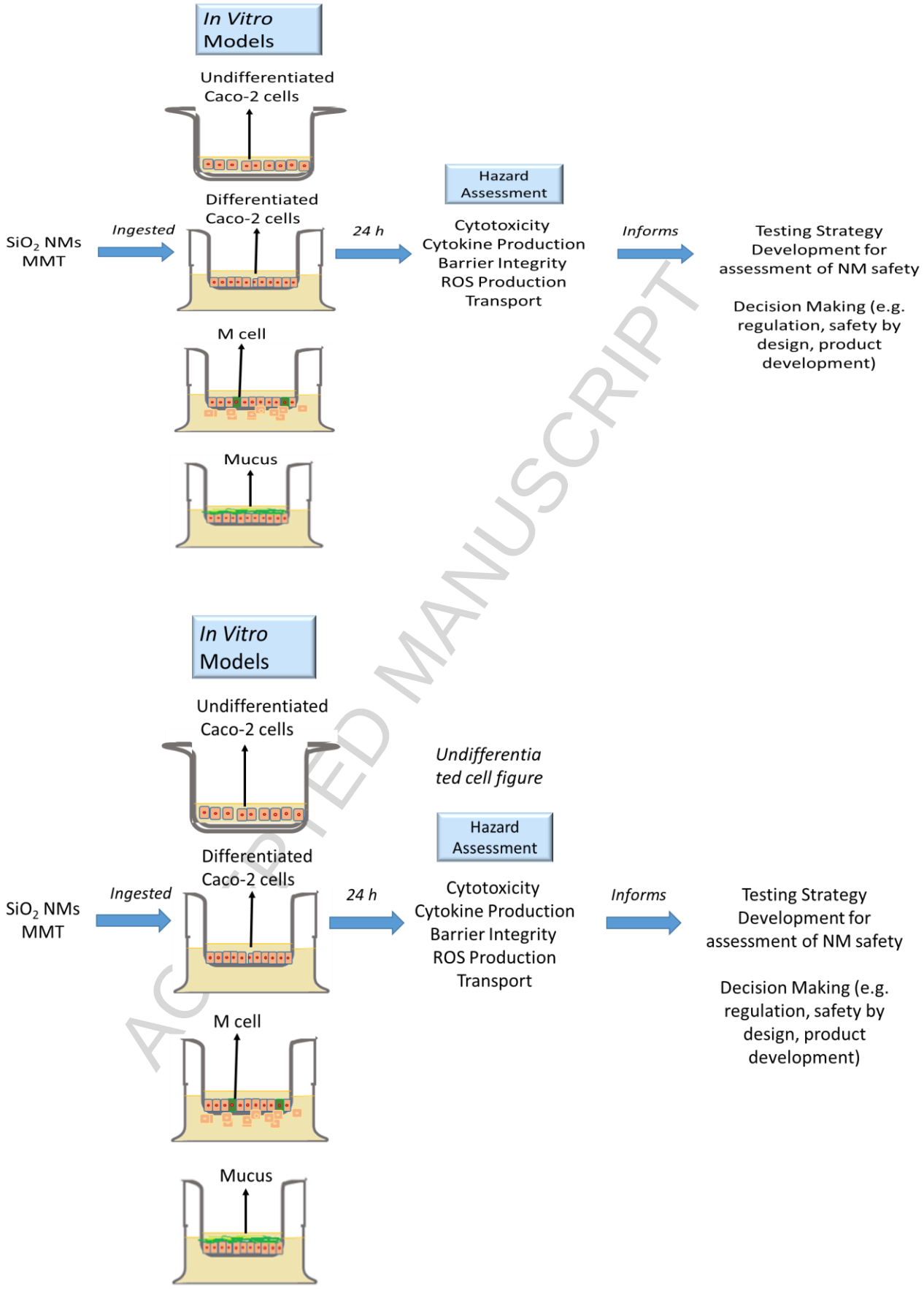

Graphical abstract

Highlights

- The toxicity of nanomaterials (NMs) that are likely to be ingested was investigated *in vitro*
- Silicon dioxide (SiO_2) NMs and Montmorillonite (MMT) did not cause cytotoxicity in intestinal models of varied complexity *in vitro*
- SiO_2 NMs and MMT did not induce reactive oxygen species production in intestinal cells *in vitro*.
- SiO_2 NMs and MMT had no impact on cell morphology of intestinal cells *in vitro.*
- SiO_2 but not MMT stimulated IL-8 production by intestinal cells *in vitro.*